Slow Dynamics of Banana-Shaped Molecules: A Theoretical Approach to Analyze ^{2}H-NMR T_2 Relaxation Times

Valentina Domenici,*,† Diego Frezzato,*,‡ and Carlo Alberto Veracini†

Dipartimento di Chimica e Chimica Industriale, Università di Pisa, Via Risorgimento 35, 56126, Pisa, Italy and Dipartimento di Scienze Chimiche, Università degli Studi di Padova, via Marzolo 1, I - 35131, Padova, Italy

Received: June 3, 2006; In Final Form: October 3, 2006

In the present work, we analyze pulsed deuterium NMR experiments performed on the isotropic and nematic phases of the banana-shaped liquid-crystalline mesogen 4-chloro-1,3-phenylene bis{4−4′-(11-undecenyloxy) benzoyloxy} benzoate (ClPbis11BB) selectively deuterated on the central ring. Starting from a previous evidence of unusual slow dynamics in the isotropic phase (Domenici V. et al., *J. Phys. Chem. B* **2005**, *109*, 769), a quantitative and model-supported analysis of the deuterium NMR data is performed here by accounting for slow-motional modulation of the magnetic anisotropies through the full solution of the stochastic Liouville equation. Focusing on the quadrupolar echo experiments performed in the nematic phase, the analysis of the transverse relaxation rate has been carried out by considering single-molecule motions and fluctuations of the local director. The main conclusions are: (a) director fluctuations are not relevant on driving the signal relaxation; (b) molecular reorientations about transverse axes control the dynamic regime of the signal relaxation and impose a full slow-motional treatment; (c) the small amplitude tumbling of the molecule within the wells of orientational potential occurs with characteristic times up to the microsecond. The outcome of our analysis has to be taken as indicative of very slow dynamics concerning out-of-plane motions of the molecules. Besides the specific application, this paper also offers the methodological tools to treat the pulsed deuterium NMR experiment in the slow-motional regime of reorientational motions and provides a detailed comparison with the usually employed fast-motional approximation.

1. Introduction

The scientific interest in the field of banana-shaped liquid crystals (BLCs)[1] is justified by several aspects covering the huge potentiality for high-tech applications[2] as well as basic and pure scientific motivations.[3−7] Among the scientific aspects, the molecular dynamics of banana-shaped molecules in their peculiar mesophases and in the isotropic phase[8] attracted the attention of several research teams.

By a simple macroscopic observation, it is well known that these systems show very high viscosity even in the isotropic phase. Moreover, several experimental results have shown unusual slow dynamics in liquid crystals of banana-shaped molecules. More interesting is that the nematic phase is affected by slow dynamics as well. In fact, several studies have confirmed the occurrence of slow dynamics in the nematic BLCs from electro-optic and electro-convection ones to measurements of some physical properties. For instance, the rotational viscosity parameter γ_1 was found to be fifty times larger in the nematic phase of a BLC than in common liquid crystals (LCs).[9]

Among the most relevant investigations, those based on deuterium NMR (DNMR) in the isotropic[7] and nematic phases[10] of a BLC sample, the 4-chloro-1,3-phenylene bis{4−4′(11-undecenyloxy) benzoyloxy} benzoate, ClPbis11BB, (Scheme 1a) show peculiar slow dynamics. A qualitative interpretation of the trend of the measured DNMR relaxation times and linewidths has been proposed by invoking a sort of molecular "entanglement". Very recently, a similar hypothesis based on the formation of small molecular "clusters", which should occur both in the isotropic and nematic phases, has been proposed by Wiant et al.[11] to explain the unusual dynamic light scattering results obtained on a very similar compound (ClPbis10BB).

The hypothesis of molecular aggregates, or equivalently of peculiar packed structures, which are unusual for common nematic phases, was also supported by further DNMR investigations.[12] These results contributed to enrich the picture of banana-shaped LCs at the molecular level, but they were not supported by a quantitative analysis based on molecular models. The present work has the main purpose to complete the previous qualitative findings by exploiting the possibilities offered by DNMR spectroscopy.

Quantitative information can be achieved by measuring low frequency-resolved T_2 by the CPMG sequence,[13] the quadrupolar and Zeeman T_1 by the Wimperis sequence,[14] or by directly analyzing the spectral line-shape and line-width to reveal dynamic processes with characteristic frequencies of the order of the quadrupolar splitting.[15]

In this work, we use data from DNMR experiments partially presented in previous reports[7,10] with specific reference to the quadrupolar echo (QE) intensities, which yield the homogeneous contribution to the spin relaxation. While the work of ref 7 was concerning the isotropic phase, here we focus mainly on measurements performed in the nematic phase. Moreover, as previously stated, the work reported in ref 7 was an explorative analysis to estimate the time scale of the dynamics affecting

* Corresponding authors. (V.D.) Phone: +39-0502219289. Fax: +39-0502219260. E-mail: valentin@dcci.unipi.it. (D.F.) Phone: +39-0498275658. Fax: +39-0498275239. E-mail: diego.frezzato@unipd.it.

† Università di Pisa.

‡ Università degli Studi di Padova.

10.1021/jp063442r CCC: $33.50
Published on Web 11/18/2006

SCHEME 1: (a) 4-Chloro-1,3-phenylene bis{4−4′-(11-undecenyloxy) benzoyloxy} Benzoate Deuterated on the Central Ring (ClPbis11BB-d_3) and (b) 3-(benzoyloxy)phenyl Benzoate Deuterated on the Lateral Rings (BOB-d_{10}). Asterisk Indicates That Position 5 Has a Very Low Percentage of Deuteration (Less than 10%).

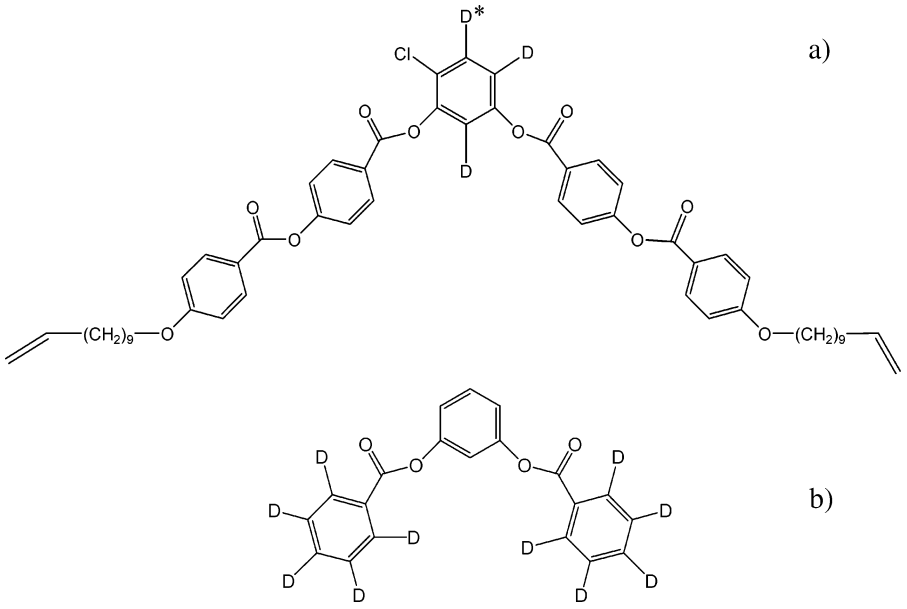

the signal relaxation, but it was not supported by a modeling of the processes and was implicitly based on the assumption of fast-motional modulation of the spectral anisotropies.[16] However, due to the emerging evidence of very slow dynamics, a separation between characteristic frequencies of motions and quadrupolar magnetic anisotropies cannot be invoked a priori. In this paper we intend to go beyond such a level of description by adopting the full slow-motional treatment in the analysis of the DNMR experiments and by modeling the dynamic processes.

On this basis, the main topics of the paper clearly emerge: (1) to establish which (slow) motions are responsible for the signal relaxation in the nematic phase, and (2) to determine their characteristic time-scales. Here we choose to focus on the nematic phase, because in this case the system can be modeled on more firm grounds. For example, pretransitional effects could play a crucial role in the isotropic phase for temperatures just above the phase transition so as to bring a further degree of arbitrariness in the modeling. However, some of the final outcomes concerning the nematic phase can be qualitatively extended also to the isotropic phase in order to establish a connection with the previous investigations.

The description of the DNMR experiments requires the specification of the time evolution of the nuclear spin density matrix through the solution of stochastic Liouville equation in the slow-motional regime.[17] All stochastic processes involving the spin-probe molecule contribute, in principle, to the signal relaxation. The relevant dynamics that we take explicitly into account are motions of the single probe-molecule (reorientations of the molecule as a whole) and collective processes (fluctuations of the local order director in the nematic phase). Simple arguments will allow us to avoid the detailed treatment of the internal motions; conformational dynamics only enters as a fast process that leaves the molecule in an average conformation subject to the slower motions.

To achieve a first level of comprehension, most of our effort concerns the invocation and justification of proper assumptions to lower the complexity of the modeling without loss of reliability. We base our analysis on the recent findings coming from the experimental investigations (on the same or on similar BLCs) about average molecular alignment[12] and magnitude of the viscoelastic parameters.[9]

This paper is structured as follows. In Analysis of DNMR Experiments, as we recall some selected DNMR measurements presented in refs 7 and 10, we build and validate the strategy for the data interpretation and perform the analysis. A quantification of the negligible contribution from director fluctuations is provided in Supporting Information, Part I. In Discussion and Conclusions, we discuss the main results, link the present inspection regarding the nematic phase to the previous analysis concerning the isotropic phase, and highlight the main items for further investigations. The Appendix is devoted to the slow-motional treatment of the QE relaxation as being caused by molecular reorientational dynamics. A detailed comparison with the fast-motional approximation is also made (technical details about the tools are provided in Supporting Information, Part II).

2. Analysis of DNMR Experiments

2.1. Preliminary Considerations. DNMR spectra of ClPbis11BB-d_3 molecules deuterated on the central ring present unusually large line-widths in both the isotropic and nematic phases.[7,10] In the isotropic phase, the line-width increases as the temperature is lowered toward the phase transition, to attain an almost constant value of about 7 kHz (the experimental error is ∼400 Hz). The three deuterons of the central ring are found to be equivalent within the spectral resolution of the single line, and such a behavior is maintained in the nematic phase within the whole temperature range of stability of the mesophase. This recently has been interpreted as evidence of a peculiar alignment of these banana-shaped molecules in the bulk nematic phase[12,18] with the central rings stabilized perpendicular to the average director (and thus to the magnetic field). The same BLC mesogen, deuterium-labeled on the four lateral aromatic rings, gives DNMR spectra with a much smaller line-broadening both in nematic and isotropic phases (up to a maximum of about 2 kHz in the nematic phase).[10,12,18] This experimental finding can be explained because the lateral aromatic rings are affected by (fast) reorientations around their para axes, which leave small

residual quadrupolar splittings and thus produce narrower line-widths. Moreover, the evaluated local order parameters agree with the picture of molecular orientation of the banana-shaped molecules presented in ref 12.

The analysis of the spectral line-width at half-height, $\Delta\nu_{h/2}$, requires consideration of all motions of the probe-molecule that yield a stochastic modulation of the quadrupolar spin Hamiltonians and, hence, contribute to the signal relaxation. In a previous work,[7] the DNMR measurements in the isotropic phase of ClPbis11BB-d_3 have been interpreted within the so-called fast-motional limit (also called motional-narrowing limit, or Redfield-limit)[16] by assuming that only fast motions are responsible for an effective "dynamic averaging" of the spin Hamiltonians. In that work, some unspecified reorientational motions of the single molecule had to be invoked as relevant processes, leading to an estimation of a unique model-free correlation time τ_{mol} of the order of $\sim 10^{-7}$ s. This is at least 2 orders of magnitude longer than that of conventional mesogens like cyano-biphenyls in the isotropic phase. On the other hand, this outcome places the DNMR relaxation in the slow-motional limit.

In fact, the resulting characteristic frequency of motion, τ_{mol}^{-1}, is not very much larger than the quadrupolar frequency $\upsilon_Q = 3e^2qQ/2h = 250$ kHz. Because the magnitude of υ_Q determines the amount of spreading of the magnetic anisotropies due to the orientational distribution of the molecular moieties carrying the deuterons, the assumption of effective dynamic averaging has to be (in principle) abandoned. In other words, some slow motions (not yet specified) place the spin relaxation between the motional-narrowing limit and the rigid-limit. If slow motions are active in the isotropic phase, the same is expected to occur in the nematic phase. A basic question then arises: which motions should be invoked in the attempt to model the monitored spin relaxation? First, the context of the specific experiments considered here has to be defined.

2.2. DNMR Relaxation Data. In the present work, we exploit pulsed DNMR experiments generating the QE signal monitored along the time axis. The QE sequence is employed to eliminate the effects of local magnetic inhomogeneities on the spin relaxation and to leave the pure homogeneous contribution from dynamics, which involves the probe molecules. The essential QE sequence is schematized by $(\pi/2)_X - \tau - (\pi/2)_Y - \tau$. The QE sequence consists of a first radiofrequency pulse that brings the nuclear spin magnetization on the transverse plane of detection. This pulse is followed by a second pulse at time τ that causes the reverse of the spin-packets and induces the refocusing of the signal, whose maximum intensity occurs at time 2τ. We start by assuming that the longitudinal relaxation (determined by the spin−lattice time T_1) is much slower than the transverse relaxation (determined by the spin−spin time T_2); hence, we focus on the latter process. This assumption will be validated a posteriori. By indicating with $I(2\tau)$ the maximum of the echo intensity occurring at time 2τ, and with $I(0)$ the intensity of the signal at the initial time just after the first radiofrequency pulse, the τ-dependent transverse relaxation rate is defined as

$$R_2^{QE}(\tau) = -\frac{1}{2\tau}\ln\frac{I(2\tau)}{I(0)} \qquad (1)$$

The analysis of the dispersion profiles of $R_2^{QE}(\tau)$ versus τ is much more informative than the direct inspection of the spectral features (especially in the case of dispersion profiles collected for different orientations of the sample with respect to the magnetic field).

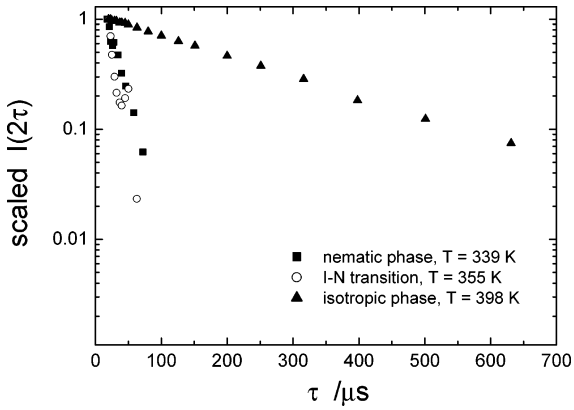

Figure 1. Experimental dependence of the maximum of the QE signal vs τ for three temperatures corresponding to nematic phase, isotropic phase, and to the transition isotropic−nematic. For a direct comparison, the signal values are scaled with respect to those at the shortest τ.

In fact, we stress the following: (1) with the QE experiment, the pure homogeneous contribution to the relaxation can be achieved; (2) a dependence of $R_2^{QE}(\tau)$ on τ implies that the spin relaxation occurs in the slow-motional regime (while the opposite is not generally true); (3) if a dependence of $R_2^{QE}(\tau)$ on τ is revealed, a model-supported analysis can provide information about the nature of the dynamic processes in terms of their specification and parametrization; and (4) in such a case, a possible additive contribution to the relaxation rate due to fast-motional dynamics can in principle be separated.

Let us focus now on the present case. QE experiments previously have been performed in isotropic and nematic phases of the ClPbis11BB-d_3 molecule. Experimental conditions and details are reported.[7,10] The maximum of the QE intensity for each spacing τ has been determined by integrating (over the frequency-range) the partially relaxed spectrum obtained by Fourier-transform of the free-induction decay sampled from time 2τ. [The same results can be obtained by using different approaches, such as taking directly the maximum intensity of the QE signal close to time 2τ.] In the following analysis, we consider only the range of τ values in which the intensities of the QE maxima vary by a factor 10. In particular, the upper value of τ ranges between 70 μs in the nematic phase (at 66 °C) and 600 μs in isotropic phase (at 120 °C). [For longer values of τ, a slight phase-mismatching of the free-induction decay sampled from time 2τ produces spurious oscillations of the QE maxima about zero; investigations to understand the origin of the phenomenon and to improve the data are currently in progress.]

Some characteristic trends are reported in Figure 1 in which (for a direct comparison) the echo intensities are scaled with respect to those values at the shortest τ. In the spirit of an explorative analysis, these data can be well fitted by a monoexponential function. Thus, in all cases, a linear fit of the logarithm of the echo intensity versus 2τ allows us to extract an experimental value of the relaxation rate, indicated with $R_{2,exp}^{QE}$, which is independent of τ.

The estimates of $R_{2,exp}^{QE}$ at several temperatures are presented in Figure 2. By taking the inverse of $R_{2,exp}^{QE}$, the (homogeneous) spin−spin relaxation time T_2 can be obtained. It should be stressed that the DNMR line-shape can be well fitted in the whole nematic range by using simple Lorentzian functions.[18] Then, as already stated in ref 7, the line-broadening is mainly due to homogeneous relaxation, because $T_2 \cong (\Delta\nu_{h/2}/\pi)^{-1}$.

The relaxation time T_2 is in the order of $\sim$40 μs in the nematic phase and longer in the isotropic phase (up to $\sim$0.4 ms at about

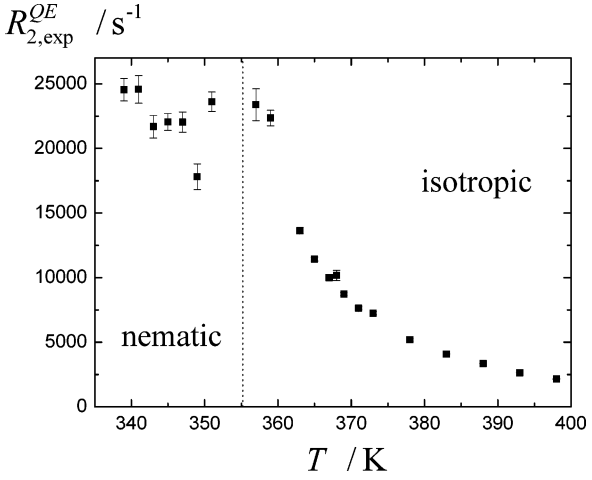

Figure 2. Temperature dependence of the transverse relaxation rate in nematic and isotropic phases, extracted from the monoexponential fits of the maximum of the QE signals vs τ. The dotted line is placed in correspondence to the isotropic−nematic transition.

40 °C above the I−N transition). Measures of the spin−lattice relaxation time yielded $T_1 \sim 30 \div 50$ ms in the nematic phase, and values up to 100 ms in the isotropic phase. Because the condition $T_1 \gg T_2$ is verified, the longitudinal relaxation process can be safely neglected, as assumed in the first approach.

2.3. Modeling the QE Experiment. To model the QE experiment, we first need to specify the relevant magnetic interactions. First, Zeeman and quadrupolar interactions have to be accounted. Then, we might consider also dipolar interactions of homo-nuclear (^{2}H−^{2}H) and hetero-nuclear (^{1}H−^{2}H) nature. The influence of dipolar couplings on the QE has been investigated, although in the rigid limit in which their effects are enhanced for both the homo-nuclear[19] and for the hetero-nuclear[20] interactions. The former are expected to have negligible effect, because the coupling constants between deuterons are of the order of only few tens of Hz. On the contrary, the latter could have an effect determining a periodic modulation of $I(2\tau)$ with a frequency of the order of the dipolar coupling constant ^{1}H−^{2}H. However, for the system under inspection, the DNMR spectra recorded with and without proton decoupling do not differ considerably.[7,10] Moreover, the QE measurements do not show any sensitivity to proton decoupling. Hence, we can assume that the deuteron−proton coupling is small enough to neglect also the hetero−nuclear interactions. Accordingly, all deuterons contribute independently, and only Zeeman and quadrupolar interactions are taken into account. On this basis, the following spin Hamiltonian is employed

$$H = \sum_i H^{(i)}, \qquad H^{(i)} = H_{\mathrm{Z}}{}^{(i)} + H_{\mathrm{Q}}{}^{(i)} \tag{2}$$

where $H_Z{}^{(i)}$ and $H_Q{}^{(i)}$ are respectively the Zeeman and quadrupolar terms for the i-th nucleus.

Because we are focusing on the transverse relaxation process, the *secular approximation* is applied. Moreover, an axially symmetric quadrupolar tensor is assumed for all deuterons. Thus we have

$$H_{\mathrm{Z}}{}^{(i)} = -\hbar\omega_{\mathrm{Z}} I_{\mathrm{Z}}{}^{(i)}\,,\; H_{\mathrm{Q}}{}^{(i)} = \hbar\omega_{\mathrm{Q}}(\theta^{(i)})(I_{\mathrm{Z}}^{(i)2} - 2/3) \tag{3}$$

in which ω_Z is the deuteron Larmor frequency,

$$\omega_{\mathrm{Q}}(\theta^{(i)}) = \frac{3\mathrm{e}^2 qQ}{4} P_2(\cos\theta^{(i)}) \tag{4}$$

$\theta^{(i)}$ is the angle formed by the specific C−D bond with the magnetic field and $P_2(x) = (3x^2 - 1)/2$ is the second-rank Legendre polynomial.

In principle, all motions that modulate the frequency-factors $\omega_Q(\theta^{(i)})$ contribute with a specific efficiency to the signal relaxation. The analysis of the signal relaxation in the isotropic phase close to the I−N transition is complicated by the lack of knowledge about the actual state of the matter at microscopic level. Pre-transitional effects, as the formation of local nematic clusters randomly oriented and subject to fluctuations of the degree of ordering, could affect the spin relaxation in a rather complex way.[11] If the isotropic averaging of the single-molecule contribution leads to a loss of details about the local dynamics, the situation in the uniform nematic phase is better defined and the signal relaxation is in principle more informative. For these reasons, we focus on the QE experiments performed in the nematic phase in the following.

The dynamics to be accounted a priori in the nematic phase at thermal equilibrium are (a) fluctuations of the local order director with respect to the average direction of alignment, (b) conformational dynamics of the molecule, and (c) reorientations of the single molecule in the nematic environment. Translational diffusion, although in principle coupled to all these motions, is neglected here (see discussion in the Supporting Information, Part I). Because of the long time scale probed by NMR, all dynamics should be modeled in the diffusive regime of motions.[21]

First, let us invoke a time-scale separation between single-molecule dynamics (b) and (c) (denoted by Mol) and slower collective processes (the director fluctuations denoted by DF). The single-molecule dynamics are assumed to occur with respect to a "frozen" local director, while fluctuations of the director itself take place in a much longer time scale. Accordingly, the transverse relaxation rate results in a sum of two contributions:

$$R_2^{\mathrm{QE}}(\tau) = R_2^{\mathrm{Mol}}(\tau) + R_2^{\mathrm{DF}}(\tau) \tag{5}$$

Separation of molecular and collective contributions in eq 5 would be in principle possible if the experiment was performed by orienting the nematic sample to a finite angle with respect to the magnetic field. In this situation, it has been demonstrated[22] that the DF contribution prevails yielding the characteristic dependence $R_2^{\mathrm{QE}}(\tau) \cong R_2^{\mathrm{DF}}(\tau) \propto \tau^{1/2}$ at large values of τ, while the contribution of the molecular motions dominates at short τ. Unfortunately, low molecular weight nematics are macroscopically aligned by the instrumental magnetic field, and in such a situation an almost τ-independent relaxation rate R_2^{DF} is predicted.[23,24] This is also the present case; in fact, angular measurements in the nematic bulk have been unsuccessful because of the fast reorientation of the molecules with respect to the magnetic field.[18] In the following, we also will show that a reasonable model for molecular reorientational dynamics may yield a basically τ-independent relaxation rate. Our experimental evidence of τ-independent relaxation rates $R_{2,\mathrm{exp}}^{\mathrm{QE}}$ supports both these models, so it is quite difficult to separate the two terms R_2^{Mol} and R_2^{DF} from the cumulative amount. Most of our efforts will concern a sensible estimation of these two contributions.

Before proceeding, we give an outlook on the methodological path that we adopt in the following. First, we quantify the contribution due to the director fluctuations alone, showing that such dynamics cannot be entirely responsible for the measured relaxation rates but could contribute up to a maximum of about 10%. Then, we focus on the molecular motions alone, trying to fit the experimental data by assuming that single-molecule

reorientational dynamics are responsible for the total amount of the relaxation rate. Finally, the outcome will impose on us a reconsideration of the collective process.

2.4. Order Director Fluctuations. The detailed analysis of the DF contribution to the relaxation rate in QE experiments is provided in the Supporting Information, Part I. Here, we summarize the main outcomes that lead us to consider such collective dynamics as irrelevant in the present case.

The theoretical description of nuclear magnetic relaxation driven by DF has been developed.[22−24] With reference to the case of average director aligned parallel to the magnetic field and to a single deuteron per molecule, a monoexponential dependence of the maximum QE signal vs τ is predicted (i.e., a τ-independent relaxation rate). Because the three deuterons of the central ring of ClPbis11BB-d_3 are basically indistinguishable from the DNMR spectrum within the resolution of the line,[12] one can analyze the data as if a single nucleus would be present.

We recall that in recent investigations[18] the spectral lineshapes could be very well fitted with a single Lorentzian function whose width is associated with homogeneous relaxation. This evidence enforces the picture of equivalent deuterons, and the view of a nematic sample well aligned with respect to the magnetic field; inhomogeneities causing distortions of the line-shape from the predicted Lorentzian are not detected.

By using the cited theoretical tools, we demonstrate first that the measured $R_{2,\mathrm{exp}}^{\mathrm{QE}}$ cannot be entirely attributed to DF (see Supporting Information). This follows a comparison between the line-widths of the quadrupolar doublet of ClPbis11BB-d_3 and those of the deuterated molecular core (BOB-d_{10}, see Scheme 1b) dissolved in the nematic phase of ClPbis11BB, not deuterated.[10] Then, an estimate of $R_2^{\mathrm{DF}}$is made by modeling the DF in well-aligned nematics according to de Gennes' theory.[25]

At the lowest level of description, only an average elastic constant (K) and an effective viscosity (η) are required to specify the angular amplitude of the DF and the correlation times associated to the independent modes of fluctuation. In particular, the effective viscosity can be identified with that damping the bending distortions of the director field.[26] A further parameter entering the modeling of the DF is the so-called short-wavelength cutoff (λ_c) of the modes, which affects both the angular amplitude of fluctuations and their shortest correlation time, τ_c. Because the time scale of the fastest fluctuation mode should meet the time scale of the single molecule tumbling in the local nematic environment, the value of $\tau_c \sim 10^{-8}$ s can be taken as a reliable guess for ordinary nematic samples.

The temperature of 340 K, which corresponds to the nematic sample far from the transition to isotropic phase, has been taken as a reference. Reliable values of the viscoelastic parameters are supplied by measures of electrical transport properties performed on a very similar compound (with C_{10} alkyl chains instead of C_{11}) in similar conditions.[9] For such a sample, the value $\gamma_1 = 1.8 \div 2.5$ Pa s was obtained for the rotational viscosity, which is very high if compared to that of typical low molecular-weight nematics. For instance, the rotational viscosity of nematic 4-methoxybenzylidene-4-butylanaline (MBBA) at 25 °C (i.e., at about 25 °C below the transition to isotropic phase) is $\sim$ 0.1 Pa s.[27] An upper limit of η can be set by using γ_1. In ref 9, the values of the elastic constants related to the splay, twist, and bend distortions are provided; from those values, we have estimated an average constant K of about 1.5 pN.

Evaluations of R_2^{DF} have been done by varying both η and K under the constraints of fixed angular amplitude of fluctuations, $\overline{\theta^2}^{1/2} = 20°$, and with τ_c shorter than 10^{-7} sec. Such a very large amplitude and the very long allowed τ_c are chosen to yield an overestimate of R_2^{DF}. In spite of this, it turns out that R_2^{DF} is limited to values below 2 kHz, and thus DF can contribute at most by 10% to the total $R_{2,\mathrm{exp}}^{\mathrm{QE}}$. Moreover, as discussed in the Supporting Information, consideration of the molecular diffusion of the probe across the sample[28] would further reduce R_2^{DF}.

On the basis of this outcome, we proceed by neglecting the DF and invoking only single-molecule dynamics. Because of the low amount of information at disposal and because of the approximations already done up to now, we shall limit the modeling of single-molecule dynamics to a minimal level of detail.

2.5. Single-Molecule Dynamics in the Nematic Phase. A comprehensive modeling of dynamics for a non-rigid molecule in the nematic phase should take into account the coupling between internal conformational motions and global reorientations in terms of hydrodynamic interactions and recoil effects.[29] We invoke a time-scale separation between internal motions and reorientations of the molecule as a whole (which are supposed to be much slower). From now on, we will completely ignore the fluctuations of the local director, and so we refer the global reorientations to the average (and macroscopically uniform) direction of alignment.

First, we consider that fast internal motions leave the molecule in an average conformation so that the molecule experiences the orientational mean-field potential of the nematic environment. We assume that the conformational dynamics contribute to the relaxation rate $R_2^{\mathrm{Mol}}(\tau)$ with a τ-independent term, $R_2^{\mathrm{conf.dyn}}$, that can be evaluated in the fast-motional limit. The slower overall reorientations are responsible for $R_2^{\mathrm{rot}}(\tau)$. Such invoked decoupling leads to $R_2^{\mathrm{Mol}}(\tau) = R_2^{\mathrm{conf.dyn}} + R_2^{\mathrm{rot}}(\tau)$. Because we consider the deuterons on the central ring of the molecule, the conformational rearrangements do not exert a relevant dynamic average of the quadrupolar Hamiltonian, and the term $R_2^{\mathrm{conf.dyn}}$ is expected to be negligible with respect to $R_2^{\mathrm{rot}}(\tau)$. Hence we consider only the reorientational motions of the molecule in its average conformation and set

$$R_2^{\mathrm{Mol}}(\tau) \equiv R_2^{\mathrm{rot}}(\tau) \tag{6}$$

The final purpose is to build a model for such dynamics and parametrize it to obtain a basically τ-independent relaxation rate, and to get $R_{2,\mathrm{exp}}^{\mathrm{QE}} \equiv R_2^{\mathrm{rot}}$.

Hereafter, we present the schematization of our modeling by recalling the assumptions already presented and provide the specific items for treating the reorientational motions (see Figure 3 for a pictorial representation of the model system):

(1) The nematic phase is uniaxial and macroscopically well oriented with average director collinear to the magnetic field.

(2) We neglect the thermal fluctuations of the local director with respect to the average direction of aligment.

(3) We invoke a time-scale separation between fast internal conformational dynamics and slower reorientational motion of the molecule as a whole, and then we neglect the former.

(4) We approximate the molecule to uniaxial symmetry. Let us introduce a molecular frame (MF) associated to the average conformation of the molecule. We assume that the principal axes of the molecular ordering tensor and of the rotational diffusion tensor (both referred to as the average conformation) are collinear. In its average conformation, the molecule is approximated to a uniaxial disk-like object from the point of view of the orientational ordering and of the rotational diffusion

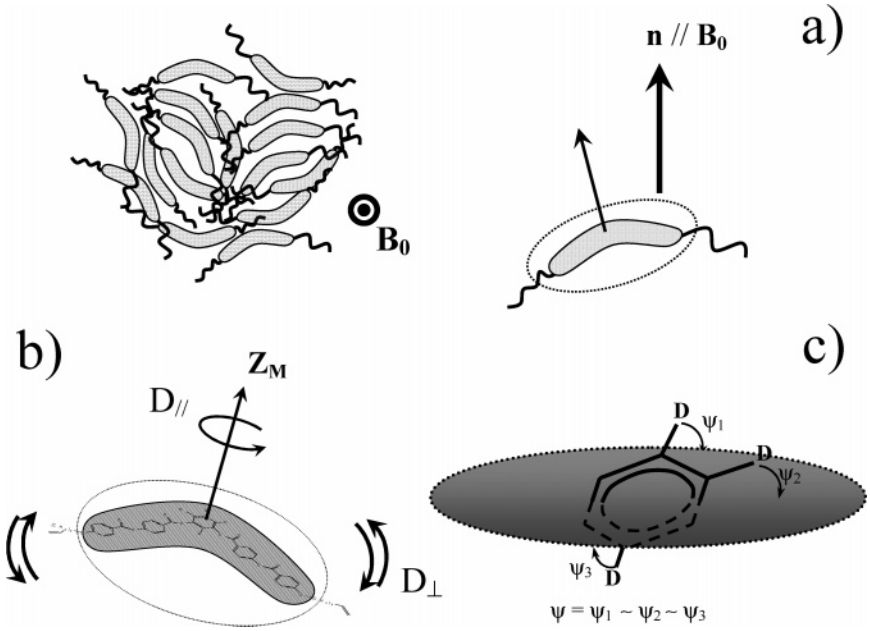

Figure 3. (a) Schematic representation of the discotic alignment in the nematic phase oriented by the magnetic field. (b) Disk-like representation of the average molecular conformation, with $\mathbf{Z_M}$ the longitudinal axis of the MF (the transverse axes are arbitrarily chosen). (c) Pictorial representation of a slight deviation of the central ring with respect to the average molecular plane; ψ denotes an average between the comparable angles formed by the C−D bonds with the molecular plane.

around the axis perpendicular to the disk's plane. We denote with $\mathbf{Z_M}$ such an axis of MF, while the transverse axes can be arbitrarily chosen. $D_{||}$ and $D_\perp$ denote the rotational diffusion coefficients for rotations about $\mathbf{Z_M}$ and about a generic transverse axis, respectively. In this picture, we completely ignore the subtle effects of the roto-translational coupling (which affects the small-steps diffusion) due to the effective bent shape of the molecule.[30] Finally, the molecular uniaxiality implies that the orientational potential experienced by the molecule only depends on the angle β between the director and $\mathbf{Z_M}$. The following basic form is adopted:

$$V(\beta)/k_B T = \epsilon[3(\cos\beta)^2 - 1]/2 \qquad (7)$$

ϵ is a phenomenological parameter that quantifies the degree of the molecular alignment.

(5) A "discotic" ordering is invoked for the molecule in its average conformation. Accordingly, $\epsilon < 0$ is required to promote the alignment of the figure axis of the molecule, $\mathbf{Z_M}$, along the director.

(6) We assume that the central ring of the molecule lies very close to the average molecular plane. (We stress that the central ring does not necessarily lie on the transverse plane of MF; the asymmetry of the molecule might favor some conformations that produce a net tilt of such a ring from the average plane.)

Assumption (1), as stated in section 2.4, is supported by recent inspections about the line shapes of the ClPbis11BB-d_3 spectrum.[18] Assumptions (2)−(4) are mostly methodological schematizations adopted to catch the features of the system with the lowest number of parameters. Assumptions (5) and (6) derive from recent experimental evidence about the molecular ordering in the bulk nematic phase of the ClPbis11BB-d_3 molecules.[12,18] In particular, no differentiation between the three deuterons could be detected from the DNMR spectrum in the entire temperature range explored. The simplest and trivial explanation, which meets such evidence, was that the central aromatic ring carrying the deuterons lies on average perpendicular (or almost perpendicular) to the magnetic field. In this way, the three nuclei have undistinguishable quadrupolar splittings within the experimental resolution. This imposes restrictions to the displacements of the central ring from the average plane: only those tilts which produce comparable and small enough angles ψ_1, ψ_2, and ψ_3 (see Figure 3c) are compatible with the data. In such a limit, an identical intermediate angle ψ will be employed in the following for the three nuclei.

Notice that the assumptions (5)−(6), and the molecular axiality invoked in (4) as well, are also here supported by the fact that the experimental profiles of $I(2\tau)$ versus τ appear to be monoexponential. In fact, since the three nuclei contribute independently to the signal relaxation, in order to detect a global monoexponential profile of $I(2\tau)$ versus τ they must be associated to very similar relaxation rates. First, this requires that they are associated to comparable order parameters (S_{C-D}). Moreover, if the biaxialiality of the molecule would be relevant in terms of alignment and/or dynamics, i.e., if preferential transverse axes of MF could be fixed, then the three nuclei would contribute differently depending on their location on the central ring. On the contrary, the experimental data are favorable to assumption (4).

The analysis of the quadrupolar splittings in ref 12 yielded a similar and negative order parameter $S_{C-D} = -0.39 \div -0.46$ for the three nuclei. Let us place the central ring coplanar to the average molecular plane, and choose the target value $S_{C-D} = -0.40$. In this situation, one gets a second-rank order parameter for the axis $\mathbf{Z_M}$, $\bar{P}_2 = -2S_{C-D} = 0.80$, which can be reproduced by eq 7 with $\epsilon = -6.0$.

At this stage, we need to evaluate $R_2^{rot}(\tau)$ as determined by single-molecule reorientations modeled according to the assumptions listed above. We need to describe the signal evolution as determined by the action of the radiofrequency pulses and by the free relaxation due to the quadrupolar interactions, modulated by the stochastic dynamics. Because the ensemble of characteristic rates of reorientational dynamics could, in principle, be overlapped to the spreading of the resonance frequencies, the analysis is based on the complete slow-motional approach. The formal description requires the solution of the stochastic Liouville equation to achieve the time evolution of

the density matrix operator for the nuclear spin system but without the usual assumption of fast-motional averaging of the magnetic anisotropies (the so-called Redfield limit).[16] However, for values high enough of the rotational diffusion coefficients, the fast-motional approximation is expected to yield an accurate description of the relaxation phenomena. While in the fast-motional limit the transverse relaxation rate is independent of τ, in the slow-motional regime some modulation of $R_2^{\mathrm{rot}}(\tau)$ vs τ, in principle, is expected (even though it might be not pronounced).

Because of the technical nature of this subject, we have concentrated the description of the tools developed to evaluate $R_2^{\mathrm{rot}}(\tau)$ according to the complete slow-motional and to the approximated fast-motional approaches in the Appendix and in the Supporting Information, Part II. In the Appendix, we also discuss the transition between the two regimes of motions and the limits of applicability of the fast-motional approach for this specific case. In particular, we demonstrate that the rate of molecular tumbling about transverse axes, $D_\perp$, mainly controls the motional regime of the signal relaxation. For the actual value of ϵ, it turns out that if $D_\perp \geq 10^6\ \mathrm{s}^{-1}$, then the fast-motional approximation provides the correct relaxation rate corresponding to a monoexponential decay of the echo intensity versus 2τ. For lower values of $D_\perp$, the full slow-motional treatment has to be adopted.

Here we use these tools to fit the target value $R_{2,\mathrm{exp}}^{\mathrm{QE}} = 22.5 \times 10^3\ \mathrm{s}^{-1}$ (see Figure 2). We start by fixing the central deuterated ring on the transverse plane of MF, which corresponds to set $\psi_1 = \psi_2 = \psi_3 = 0°$. Calculations of R_2^{rot} have been performed for $\epsilon = -6.0$ and by varying independently $D_{\|}$ and $D_\perp$ in the range $10^2 \div 10^9\ \mathrm{s}^{-1}$. The pairs of values leading to the smallest deviation from the target relaxation rate (and in any case, not larger than 15%) have been retained. A restriction about $D_{\|}/D_\perp$ might be imposed based on the ratio of the disk-like molecule under assumption of validity of the Stokes−Einstein relation for rotational diffusion in a homogeneous viscous environment.[30] However, this would introduce a further arbitrariness concerning the choice of such a ratio. Moreover, because the possible entanglement at the molecular level that may alter the mechanism of small-steps diffusion, we prefer to relax such a constraint and to leave the two coefficients independent of each other. By exploiting the investigations presented in the Appendix, the full slow-motional treatment has been employed only for $D_\perp \leq 10^6\ \mathrm{s}^{-1}$, while the less burdensome fast-motional treatment has been adopted for higher values of the diffusion coefficient. The outcome is reported with full circles in Figure 4. A good fit with data is realized when $D_\perp$ ranges within a narrow interval (in the range $10^3 \div 10^4\ \mathrm{s}^{-1}$), while the $D_{\|}$ results only bounded below $10^5\ \mathrm{s}^{-1}$.

Although the situation of central ring coplanar to the transverse MF plane should be taken as the reference in absence of further information, the matching procedure has been repeated by allowing a small tilt of C−D bonds. To keep the spectral quadrupolar splitting unaltered, that is, to maintain $S_{\mathrm{C-D}} = -0.40$, the intensity of the mean field potential has been modified to yield the correct value of the order parameter: $\bar{P}_2 = 2S_{\mathrm{C-D}}/(3\ \sin^2\ \psi\ -1)$ for the alignment of the axis $\mathbf{Z_M}$. Calculations have been done for the average angle $\psi = 10°$, which requires $\epsilon = -8.7$ to get $\bar{P}_2 = 0.88$. The outcome of the fit is presented with open circles in Figure 4. It appears that the ring's tilt extends the range of variation of both the diffusion coefficients. Roughly speaking, faster reorientational dynamics are allowed under the condition $R_2^{\mathrm{rot}} = R_{2,\mathrm{exp}}^{\mathrm{QE}}$. A qualitative explanation of this fact can be found by examining how the orientation-dependent quadrupolar frequency, whose stochastic modulation is responsible for the signal relaxation, is related to ψ. Elaboration of eq 9 in the Appendix leads to see that even at fixed (average) spectral splitting, the (instantaneous) orientation-dependent quadrupolar frequency has components whose magnitude vary as $\sim\sin\psi$; hence, they increase as ψ increases. This implies that the same reorientational dynamics of the molecule (in terms of geometry of motion and time scales) would produce a larger line-width, that is, a higher R_2^{rot} in our context. On the other way round, to reduce R_2^{rot} and still obtain the target value $R_{2,\mathrm{exp}}^{\mathrm{QE}}$, the dynamics has to be speeded up with respect to the situation of no tilt of the central ring.

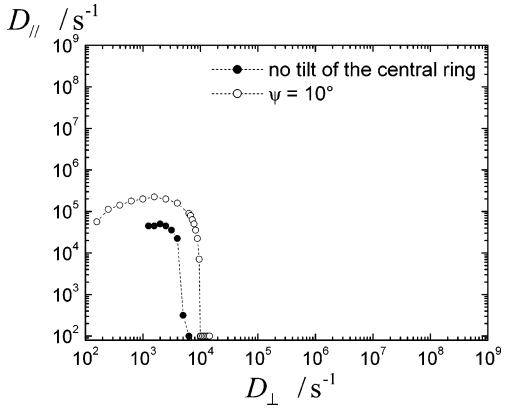

Figure 4. Values of diffusion coefficients for rotations about the molecular figure axis ($D_{\|}$) and about transverse axes ($D_\perp$), which yield $R_{2,\mathrm{exp}}^{\mathrm{QE}} = R_2^{\mathrm{rot}}$ within 15% tolerance (the target value is $R_{2,\mathrm{exp}}^{\mathrm{QE}} = 22.5 \times 10^3\ \mathrm{s}^{-1}$). Full circles refer to the deuterated ring coplanar to the average molecular plane, open circles refer to an average tilt of the C−D bonds: $\psi = 10°$. The same order parameter $S_{\mathrm{C-D}} = -0.40$ has been employed in both situations, by using the value $\epsilon = -6.0$ for the orientational potential in the former case and $\epsilon = -8.7$ in the latter case.

Finally, we stress that up to now we have considered only the target order parameter $S_{\mathrm{C-D}} = -0.40$ chosen in the experimental interval of values.[12] Explorative calculations have been performed for the higher value $S_{\mathrm{C-D}} = -0.42$ (corresponding to $\epsilon = -7.0$) and by assuming no tilt of the central ring. The outcome (profile here not shown) reveals that the increase of the discotic order leads to get $R_2^{\mathrm{rot}} = R_{2,\mathrm{exp}}^{\mathrm{QE}}$ with slightly lower values of the diffusion coefficients, that is, it has the opposite effect than the tilt of the central ring. Still, in a qualitative way, this can be explained by taking into account that the higher degree of alignment speeds up the small-amplitude tumbling of the molecule about the director (see the discussion in the Appendix). Hence, the required value of the relaxation rate is achieved with lower values for the diffusion coefficients.

Summarizing, it emerges that the experimental transverse relaxation in the nematic phase can be interpreted by means of single-molecule reorientations. However, we must admit that the analysis contains several degrees of arbitrariness (possible tilt of the central ring, order parameter of the C−D bonds). In spite of this, we can provide reliable upper limits for the rotational diffusion coefficients: $D_\perp$, which is related to out-of-plane molecular rotations, is limited below $\sim 10^4\ \mathrm{s}^{-1}$, while $D_{\|}$, which is related to the spinning about the figure axis, is bounded by $\sim 10^5\ \mathrm{s}^{-1}$.

Furthermore, because we find $\mathrm{D}_\perp \ll 10^6\ \mathrm{s}^{-1}$, it emerges that the signal relaxation requires the complete slow-motional approach. We remark that the impossibility to fix the diffusion coefficients in a more strict way is due to the fact that only a

single value $R_{2,exp}^{QE}$ has to be reproduced by varying two parameters ($D_\perp$ and $D_{||}$). Our rough model, which approximates the molecule to a uniaxial disk-like object, is even much too sophisticated with respect to the amount of information at disposal.

Notice that even the upper value of $D_\perp$ is more than 2 orders of magnitude lower than that of molecules of similar size in common low molecular-weight nematic liquid crystals.[31,32]

Once $D_\perp$ is specified, one can estimate the characteristic times of different molecular reorientations from the analysis of the eigenvalues of the diffusion operator (see the Appendix): the flipping process (corresponding to a full reorientation of the figure axis), the molecular tumbling (small-amplitude reorientations of the molecule), and the molecular spinning about the figure axis. Becuase of the nematic environment forcing the molecule to lie on the plane perpendicular to the director, the flipping process requires to cross a mean-field potential barrier that causes the well-known slowdown of such a motion with respect to the free-rotation case. Such a process is related to the lowest not-null eigenvalue, which yields $\tau_{flip} = (6.6 \times 10^{-3} D_\perp)^{-1}$ for the actual energy barrier of $3|\epsilon|/2 = 9\ k_B T$ units. Even the highest value of $D_\perp$ obtained by the matching procedure would place the molecular flipping among ultraslow processes in the time scale of several milliseconds. However, because the flipping does not modulate second-rank rotational functions, DNMR is insensitive to such a motion (while other techniques sensitive to modulation of first-rank properties, like dielectric relaxation, could be informative on it). Hence, the signal relaxation is driven by faster small-amplitude tumbling within the wells of the orientational potential and by in-plane rotations of the molecules about the figure axes. These motions are tightly coupled and are associated to a collection of characteristic times that are ϵ-dependent. However, from the ensemble of eigenvalues of the diffusion operator, the slowest component associated with the "pure" tumbling can be evaluated. For $\epsilon = -6.0$, the slowest component is associated with the longest characteristic time $t_{tumbl.} = (14.1\ D_\perp)^{-1}$. With the estimated upper limit for the diffusion coefficient, $t_{tumbl.}$ is of the order of $1 \div 10\ \mu$s.

The outcome of such long time-scales of molecular motions, which are unexpected in common thermotropic liquid crystals, might suggest that relevant features have been neglected in the modeling. In particular, as discussed in the next section, the resulting very slow out-of-plane reorientations render questionable the invoked time-scale separation between single-molecule dynamics and order director fluctuations. This demands for a reconsideration of the collective process.

3. Discussion and Conclusions

In the previous section, we faced the problem of interpreting the QE NMR relaxation data in the nematic phase of the ClPbis11BB-d_3 molecules deuterated on the central ring. The following information was at our disposal, arising from the present measurements and from recent analyses on the same material[7,12,18] and on a very similar liquid crystal:[12,33]

(1) A basically τ-independent transverse relaxation rate, $R_{2,exp}^{QE}$, of about 22.5×10^{-3} s^{-1} insensitive to temperature variations within the nematic phase.[7,10]

(2) Evidence of "discotic" alignment of the molecules with the central aromatic ring perpendicular to the magnetic field and an estimate of the average order parameters for the three C−D bonds.[12]

(3) An estimate of quadrupolar splittings and line-widths for the deuterated core's moiety (BOB-d_{10}) diluted in the nematic ClPbis11BB.[10]

The analysis of the transverse relaxation rate $R_{2,exp}^{QE}$ extracted from the QE experiments has been carried out by considering single-molecule and collective dynamics (fluctuations of the local director), which in principle can modulate the quadrupolar magnetic anisotropies in the slow-motional regime. Most of the effort concerned the control of several approximations applied with the purpose to lower the complexity of the model to the basic amount of information at disposal without the loss of reliability. A sequence of assumptions has led us to focus only on molecular reorientations about the local director and on fluctuations of the director itself with respect to the average direction of alignment (which is collinear to the magnetic field). Moreover, a decoupling between these two processes has been initially assumed based on the time-scale separation usually invoked among molecular and much slower collective processes.

Besides the items (1)−(3) listed above, our analysis also invoked the assumption of uniform nematic phase with average macroscopic director well oriented with respect to the magnetic field: possible permanent inhomogeneities of the sample have been ignored. On the other hand, the observed unusually large line-width, in principle, could have several origins: (i) inequality of the three central deuterons; (ii) static distortions of the sample; and (iii) very slow dynamics.

In the present work, we have shown that the interpretation (iii) can account for the experimental data, because some relevant motions result too slow to be placed close to the rigid limit on the DNMR time-scale. Moreover, the situations (i) and (ii) would produce some (not observed) strong deviations from the monoexponential dependence of the maximum QE intensity vs τ, and ultimately a deviation of the spectral line-shapes from the Lorentzian profile. From the features of the DNMR spectra,[12] because of well fitting of the line-shapes by using a single Lorentzian function,[18] we can exclude the cases (i) and (ii).

Among the most relevant results, the analysis of $R_{2,exp}^{QE}$ has led us to exclude the relevance of the director fluctuations. However, the subsequent attempt to account for $R_{2,exp}^{QE}$ by considering only molecular reorientations in the nematic environment revealed that very slow dynamics need to be invoked. To fit the experimental data, a rough model was used that treats the molecule as a disk-like object. In spite of such a picture, we could reach a first level of specification about the reorientational motions that drive the spin relaxation in terms of their assignment (i.e., kind of motions) and the estimate of the corresponding time scales.

To summarize, we have found that (a) the diffusion coefficient $D_\perp$ related to the molecular tumbling mainly controls the dynamic regime of the signal relaxation, and the full slow-motional treatment is necessary to interpret the present data, (b) only upper limits of the rotational diffusion coefficients could be estimated, with $\sim 10^4$ s^{-1} as the upper limit for $D_\perp$, and (c) the small-amplitude tumbling of the molecule within the wells of the orientational potential should occur with very long characteristic times up to the microsecond scale.

On the other hand, such slow tumbling dynamics imposes a reconsideration of the director fluctuations as coupled to the single-molecule motions. Even in the case of decoupling still invoked, the estimate of R_2^{DF} presented in the Supporting Information, Part I could be reviewed by allowing for the shortest relaxation time of fluctuations (τ_c), even larger than the microsecond. This would increase the contribution of the DF to the relaxation rate. Although we have established that the DF alone cannot account for the QE relaxation, for the peculiar system under inspection it seems to be hard to

distinguish between tumbling of the single molecule about the local director and short-range fluctuations of the director itself.

For all these reasons, the outcome of our analysis has to be taken mainly as indicative of very slow dynamics concerning out-of-plane motions of the molecules.

It is worth noting that evidence of slow molecular reorientations also emerged from the analysis of the DNMR line-width in the isotropic phase of the same compound. In ref 7, the DNMR data were interpreted in the fast-motional regime by invoking a single process associated to an (average) correlation time, estimated of the order of $\sim 10^{-7}$ s at 10 °C above the I−N transition. To interpret such unusual slow dynamics, it was made the conjecture that peculiar interactions among the banana-shaped molecules (entanglements) impede rotations about the long axes. If so, such a constraint due to local packing is expected to be present also in the nematic phase. Indeed, the very slow tumbling motions pointed out in this work are compatible with such expectation. Our slow-motional and model-supported analysis confirms that the slow dynamics invoked in ref 7 should be attributed to out-of-plane rotations of the molecule.

Further developments in understanding the origin of these restricted motions will require to take into account the local structures formed by the bent molecules both in isotropic and nematic phase. To this aim, the recent hypothesis of entanglement,[7] as well as molecular clustering,[10] seems to offer a possible way to investigate.

Finally, this study will be extended to additional two isotopomers of the same sample ClPbis11BB, deuterium labeled on the four lateral phenyl rings, to achieve information about the internal dynamics and to get more evidence of the slow overall molecular motions.

Acknowledgment. The authors thank the Italian MIUR for finantial support (P.R.I.N. 2005). V.D. and C.A.V. thank Professor Katalin Fodor-Csorba for the deuterated banana-shaped ClPbis11BB sample and Professor Bostjan Zalar for helpful suggestions. The authors are grateful to Professor Giorgio J. Moro for discussions, helpful advice, and suggestions.

Appendix

Let us consider a probe-molecule carrying a single deuteron and reorienting in the uniaxial nematic phase (the label *i*, used in the main text to specify different deuterons, is dropped out from now on). Here, we outline the tools to evaluate the maximum intensity of the (normalized) QE signal and the corresponding relaxation rate for a chosen τ, that is $I(2\tau)/I(0)$ and $R_2^{\mathrm{rot}}(\tau)$ respectively, as determined by reorientational dynamics of the single-molecule. We start by considering the complete slow-motional treatment, then we provide the expression for the τ-independent relaxation rate that is recovered in the fast-motional (Redfield) limit. Finally, these tools will be used to compare the predictions of slow-motional and fast-motional approaches, to establish the limits of applicability of the latter and to support the choices made for the data analysis in section 2.

We consider cylindrical symmetry of the quadrupolar tensor and introduce the quadrupolar frame (QF) whose longitudinal axis is taken along the C−D bond, while the transverse axes are arbitrarily chosen. Then, we introduce a laboratory frame (LF) with the longitudinal axis collinear to the magnetic field B_0. By focusing on the transverse relaxation of the signal, the quadrupolar Hamiltonian is approximated by retaining only the secular terms:

$$H_Q/\hbar = \omega_Q(I_z^2 - 2/3)\,, \qquad \omega_Q = f\,\mathrm{D}^2_{0,0}(\Omega^0_Q) \tag{8}$$

I_z is the component of the nuclear spin operator along the magnetic field, $f = 3e^2qQ/4\hbar = \pi\nu_Q$ being ν_Q the quadrupolar frequency, and Ω^0_Q is the set of Euler angles,[34] which identifies the QF with respect to the LF. $D^j_{m,k}(\alpha,\beta,\gamma) = e^{-im\alpha}d^j_{m,k}(\beta)e^{-ik\gamma}$ is a rotational Wigner function, with $d^j_{m,k}(\beta)$ being a "reduced" Wigner function.[34] In particular, the second-rank one entering eq 8 coincides with the Legendre polynomial, $P_2(\cos\theta)$ in which θ is the angle between the C−D bond and the magnetic field. Let us now introduce the average director frame (ADF) with the longitudinal axis along the (average) director, while the transverse axes can be arbitrarily chosen becuase of the uniaxiality of the phase. θ_B denotes the angle between B_0 and the average director. Finally, we consider a molecular frame (MF) tethered to the molecule. In our basic model, we assume that the molecule in its average conformation (as resulting from fast internal motions) can be treated as a disk-like object from the points of view of the equilibrium orientational distribution in the nematic environment and of the rotational dynamics. Accordingly, the axis $\mathbf{Z_M}$ of MF is taken perpendicular to the average molecular plane, while the transverse axes can be arbitrarily fixed. The transformations among the several frames are schematized as

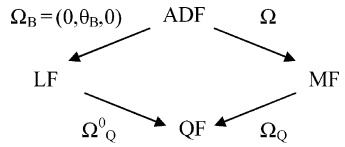

in which the rotations are specified by sets of Euler angles. In particular, Ω specifies the molecular orientation with respect to the ADF. Then, $\Omega_Q = (\alpha_Q, \beta_Q, 0)$ individuates the C−D bond with respect to the MF axes (to establish a connection with Figure 3c, the angles ψ_i are given by $\pi/2-\beta_Q$ for the specific nucleous). Finally notice that the choice $\Omega_B = (0, \theta_B, 0)$ fixes the transverse axes of LF once those of ADF have been chosen.

In the general situation of average director not collinear to the magnetic field (i.e., for $\theta_B \neq 0$), the orientation-dependent frequency ω_Q is expanded as:

$$\omega_Q(\Omega) = \sum_{M,K=-2}^{+2} \sigma_{M,K}\mathrm{D}^2_{M,K}(\Omega), \qquad \sigma_{M,K} = f\,d^2_{M,K}(\theta_B)D^2_{M,K}(\Omega_Q) \tag{9}$$

Such a form shows that molecular reorientations cause a (stochastic) modulation of the quadrupolar Hamiltonian through the modulation of the frequency factor $\omega_Q(\Omega)$ and thus contribute to the signal relaxation.

The signal evolution during the quadrupolar-echo (QE) experiment is described by the stochastic form of the Liouville equation,[17] which defines the time evolution of the density matrix operator for the nuclear spin states in the case of stochastic modulation of the resonance frequencies. Moreover, one has to consider the radiofrequency pulses, which produce "instantaneous" and selective rotations of the spin packets. Although such an approach is quite general regardless of the motional regime, we refer to it as the "slow-motional" approach.

The slow-motional description of the QE sequence and of the extended Carr−Purcell−Meiboom−Gill sequences has been carried out in refs 22−24. Although the context was different, namely, the dynamics responsible for the spin relaxation were

the fluctuations of the local director rather than single-molecule reorientations, the basic expression for the maximum echo's intensity at time 2τ holds in all generality; by adapting it to the present case we have

$$I(2\tau)/I(0) = \int \mathrm{d}\Omega\ \mathrm{e}^{-U^*\tau}\ \mathrm{e}^{-U\tau}\ p_{\mathrm{eq}}(\Omega), \qquad U = i\omega_{\mathrm{Q}}(\Omega) + \Gamma_{\Omega} \tag{10}$$

where the integration over the Euler angles is specified by $\int d\Omega(...) \equiv \int_0^{2\pi} d\alpha \int_0^{\pi} d\beta \sin\beta \int_0^{2\pi} d\gamma\ (...)$. In eq 10, U is an evolution operator acting on the variable Ω and made of two contributions: a complex-frequency factor $i\omega_{\mathrm{Q}}(\Omega)$, related to the spreading of the resonance frequencies due to the distribution on Ω, summed to the operator Γ_{Ω} (having physical dimension of a frequency), which defines the rates of stochastic modulation of these magnetic anisotropies. More precisely, Γ_{Ω} describes the evolution of the nonequilibrium distribution $p(\Omega,t)$ through

$$\frac{\partial}{\partial t}p(\Omega,t) = -\Gamma_{\Omega}p(\Omega,t), \qquad \lim_{t\to\infty} p(\Omega,t) = p_{\mathrm{eq}}(\Omega) \tag{11}$$

being $p_{\mathrm{eq}}(\Omega)$ the Boltzmann distribution at thermal equilibrium. Because the nuclear magnetic relaxation probes motions in the long time scale beyond the nanosecond, the following Smoluchowski form of Γ_{Ω} for rotational diffusive dynamics[21] is adopted:

$$\Gamma_{\Omega} = \mathbf{M}^{\dagger} p_{\mathrm{eq}}(\Omega)\mathbf{D_R}\mathbf{M} p_{\mathrm{eq}}(\Omega)^{-1} \tag{12}$$

where $\mathbf{M}$ is the operator of infinitesimal rotations about the molecular axes, with $\mathbf{M}^{\dagger} = -\mathbf{M}^{\mathrm{Tr}}$ its adjoint, and $\mathbf{D_R}$ is the rotational diffusion tensor expressed in the MF.

According to the assumption of disk-like molecules in uniaxial nematic phase, the equilibrium orientational distribution only depends on the angle β between the figure axis and the director. We model such a distribution as

$$p_{\mathrm{eq}}(\Omega) = \frac{\mathrm{e}^{-V(\Omega)/k_{\mathrm{B}}T}}{\int \mathrm{d}\Omega\ e^{-V(\Omega)/k_{\mathrm{B}}T}}, \ V(\Omega)/k_{\mathrm{B}}T = \epsilon D^2_{0,0}(\Omega) \tag{13}$$

with $V(\Omega)$ the mean-field orientational potential acting on the molecule. Moreover, the rotational diffusion tensor is uniaxial in the MF:

$$\mathbf{D_R} = \begin{pmatrix} D_{\perp} & 0 & 0 \\ 0 & D_{\perp} & 0 \\ 0 & 0 & D_{\parallel} \end{pmatrix} \tag{14}$$

By employing the following symmetrized form of the operator

$$\tilde{\mathbf{U}} = p_{\mathrm{eq}}(\Omega)^{-1/2}[i\omega_{\mathrm{Q}}(\Omega) + \Gamma_{\Omega}]p_{\mathrm{eq}}(\Omega)^{1/2} = i\omega_{\mathrm{Q}}(\Omega) + \tilde{\Gamma}_{\Omega} \tag{15}$$

eq 10 changes to

$$I(2\tau)/I(0) = \int \mathrm{d}\Omega\ p_{\mathrm{eq}}(\Omega)^{1/2}\ \mathrm{e}^{-\tilde{U}^*\tau}\ \mathrm{e}^{-\tilde{U}\tau}\ p_{\mathrm{eq}}(\Omega)^{1/2} \tag{16}$$

Such an integral can be interpreted as a Hermitian scalar product on the space of the Euler angles, and it can be expanded into the following ortho-normal basis of functions:

$$|j,m,k\rangle = \left(\frac{2j+1}{8\pi^2}\right)^{1/2} D^{\mathrm{j}}_{\mathrm{m},k}(\Omega)\ , \qquad \langle j,m,k|j',m',k'\rangle = \delta_{j,j'},\delta_{m,m'},\delta_{k,k'} \tag{17}$$

where with the standard *bra-ket* notation, the complex-conjugation of the *bra-* functions is implicit. We remark that the eigenvalues of the pure diffusive problem, that is, those of the operator $\tilde{\Gamma}_{\Omega}$ alone, are the characteristic frequencies of the reorientational process. In the case of free rotational diffusion, the basis elements $|j,m,k\rangle$ are eigenfunctions of $\tilde{\Gamma}_{\Omega}$ with eigenvalues: $\gamma_{j,m,k} = j(j+1)D_{\perp} + k^2(D_{\parallel} - D_{\perp})$. The orientational potential perturbs such a situation mainly causing the well-known slowdown of the full reorientation of the molecular figure axis (the so-called flipping process associated to the lowest not-null eigenvalue), because the energy barrier has to be crossed. On the contrary, for high-enough potential's strength, the tumbling motions of the molecules (i.e., the small-angle reorientations of the figure axis within the wells of potential) are speeded up.

Upon the chosen basis of functions, the matrix representation $\tilde{\mathbf{U}}$ of the operator in eq 17 is a general complex-not-symmetric matrix. The derivation of the matrix $\tilde{\mathbf{U}}$ and the explicit expression of its elements are provided in the Supporting Information, Part II.

By diagonalizing $\tilde{\mathbf{U}}$, after some algebra one gets:

$$I(2\tau)/I(0) = \sum_{N,N'} w_{N,N'}\ \mathrm{e}^{-(\lambda_N{}^*+\lambda_{N'})\tau}, \qquad w_{N,N'} = [\mathbf{v}^{\dagger}(\mathbf{X}^{-1})^{\dagger}]_N(\mathbf{X}^{\dagger}\mathbf{X})_{N,N'}[\mathbf{X}^{-1}\mathbf{v}]_{N'} \tag{18}$$

where $N \equiv (j,m,k)$ is a cumulative index which labels the basis elements, $\mathbf{X}$ is the eigenvectors matrix such that $\tilde{\mathbf{U}}\mathbf{X} = \mathbf{X}\Lambda$, and λ_N are the eigenvalues. (Notice that since the matrix $\tilde{\mathbf{U}}$ does not commute with its adjoint, in general $\mathbf{X^{-1}} \neq \mathbf{X}^{\dagger}$ and the inversion of the matrix $\mathbf{X}$ cannot be avoided unless in the case of special symmetries about $\tilde{\mathbf{U}}$.) Moreover, $\mathbf{v}$ is a vector with elements: $v_N = \langle p_{\mathrm{eq}}(\Omega)^{1/2}|N\rangle$. Finally, from the (zero-time normalized) QE intensity, the homogeneous relaxation rate is obtained as:

$$R_2^{\mathrm{rot}}(\tau) = -\frac{1}{2\tau}\ln\frac{I(2\tau)}{I(0)} \tag{19}$$

We stress that procedure outlined above holds for arbitrary angles θ_{B}. However, the relevant experimental case for low molecular-weight materials is $\theta_{\mathrm{B}} = 0$, because the instrumental magnetic field is strong enough to orient the sample. In this situation, the matrix $\tilde{\mathbf{U}}$ becomes diagonal on the index m; in fact $\tilde{\Gamma}_{\Omega}$ is always diagonal on m, and the representation of $i\omega_{\mathrm{Q}}(\Omega)$ also becomes diagonal on m because only the factors $\sigma_{0,K}$ in eq 9 are not-null. Because the elements of $\mathbf{v}$ do not vanish only if $m = 0$ (and $k = 0$ as well), we can directly select the corresponding matrix block and work with the reduced basis set $|j,0,k\rangle$ of much smaller dimension. A further simplification concerning the case $\theta_{\mathrm{B}} = 0$ comes by exploiting the molecular uniaxiality. This assumption allows us to choose arbitrarily the transverse axes of MF. By fixing the x-axis parallel to the projection of the C−D bond on the transverse plane of MF, we set $\alpha_{\mathrm{Q}} = 0$. This implies that the factors $\sigma_{0,K}$ are real, and thus the matrix $\tilde{\mathbf{U}}$ results to be complex-symmetric. In such a special case, one realizes that $\mathbf{X^{-1}} \equiv \mathbf{X}^{\mathrm{Tr}}$, therefore the time-consuming inversion of the matrix $\mathbf{X}$ can be avoided.

Now we turn to the evaluation of the transverse relaxation rate in the limit of fast motions (Redfield limit).[16] In such a situation, a τ-independent relaxation rate (associated to a mono-expenential decay of the echo intensity vs 2τ) is found. By means of a perturbative treatment of the stochastic Liouville equation, one finds the well-known result that all information about the signal relaxation driven by the stochastic dynamics

is contained in the spectral density of the self-correlation function of the modulated spin Hamiltonian (over $\hbar$):

$$J_Q(\omega) = \int_0^\infty dt\, e^{-i\omega t}\overline{\delta\omega_Q(0)\delta\omega_Q(t)} \qquad (20)$$

where $\delta\omega_Q = \omega_Q - \overline{\omega_Q}$ denotes the fluctuating part with respect to the equilibrium average. A proper linear combination of $J_Q(\omega)$ values, specified at different sampling frequencies, yields the relaxation rate.[35] According to the secular approximation applied to the quadrupolar Hamiltonian, that is, in the "adiabatic" limit, only the zero-frequency contribution is relevant and one finds $R_2^{rot} \equiv J_Q(0)$.

Making use of the symmetrized diffusion operator, the required correlation function can be written in the form:

$$\overline{\delta\omega_Q(0)\delta\omega_Q(t)} = \langle p_{eq}(\Omega)^{1/2}\delta\omega_Q(\Omega)|e^{-\tilde{\Gamma}_\Omega t}|p_{eq}(\Omega)^{1/2}\delta\omega_Q(\Omega)\rangle \qquad (21)$$

By expanding such an integral on the basis functions (eq 17), and then diagonalizing the matrix $\tilde{\Gamma}_\Omega$, one gets:

$$\overline{\delta\omega_Q(0)\delta\omega_Q(t)} = \sum_N \tilde{w}_N e^{-\gamma_N t}, \qquad w_N = |(\mathbf{R}^{Tr}\tilde{\mathbf{v}})_N|^2 \qquad (22)$$

where $N \equiv (j,m,k)$, the vector $\tilde{\mathbf{v}}$ has elements $\tilde{v}_N = \langle N|p_{eq}(\Omega)^{1/2}\delta\omega_Q(\Omega)\rangle$, $\mathbf{R}$ is the matrix of the eigenvectors of $\tilde{\Gamma}_\Omega$, and γ_N are the eigenvalues. By inserting eq 22 into eq 20 evaluated at zero-frequency:

$$\text{fast motional limit: } R_2^{rot} = \sum_N \tilde{w}_N/\gamma_N \qquad (23)$$

As already stressed in the context of the slow-motional approach, in this case also the reduced basis set $|j,0,k\rangle$ can be used if $\theta_B = 0$.

FORTRAN codes have been written to evaluate $I(2\tau)/I(0)$ and $R_2^{rot}(\tau)$ in the slow-motional case (see eqs 18 and 19) for several τ values, and the constant R_2^{rot} in the fast-motional case (see eq 23). The relevant situation $\theta_B = 0$ has been considered with generic input about the angle β_Q, the potential's strength-parameter ϵ, $D_{||}$, and $D_\perp$. Convergence of the calculations has to be achieved with respect to the extension of the set of basis functions, which is determined by the maximum rank j_{max}. Convergence is considered reached if the values of the relaxation rate do not vary more than 0.1% to a further extent of j_{max}. Double-precision handling of digits has been adopted.

Summarizing, we have at disposal two different tools to evaluate the transverse relaxation rate in the QE experiment: the complete slow-motional approach and the fast-motional approximation. The former should reduce to the latter for high enough values of the rotational diffusion coefficients, which control the efficiency of the dynamic averaging of the magnetic anisotropies in the different regimes of motion. The recovery of the fast-motional limit from the slow-motional approach has been used first to check the consistency of the tools. Then, such an analysis directly shows in which dynamic range the deviations from the (usually employed) fast-motional approximation become so relevant as to require the full treatment.

We have done this inspection for $\epsilon = -6.0$ and for several values of $D_{||}$, $D_\perp$ spanning the range 10^2-10^9 s^{-1}. First, the C−D bond has been set to lie on the average molecular plane. This corresponds to set $\beta_Q = \pi/2$ in eq 9. Moreover, the selected range of τ values is $10^{-5} \div 10^{-4}$ s. Notice that both ϵ and the range of τ chosen here are the same considered in the data analysis of section 2. The outcome of the calculations is summarized in Figure 5. The empty circles refer to situations for which $R_2^{rot}(\tau)$ obtained by the slow-motional treatment results independent of τ (or only slightly dependent on it) and coincident within 1% with the value from the fast-motional approach. The full circles indicate quantitative deviations from the fast-motional prediction, that is, when a marked dependence of $R_2^{rot}(\tau)$ vs τ is found, and its average value (over the considered range of τ) also deviates more than 5% from R_2^{rot} evaluated in the fast-motional approximation. Notice that for $D_\perp \geq 10^6$ s^{-1}, regardless of the value of $D_{||}$, the fast-motional approximation provides an accurate estimate of the (constant) relaxation rate. For $D_\perp = 10^5$ s^{-1} the fast-motional approach begins to fail. However, a direct look at the profiles of $R_2^{rot}(\tau)$ vs τ (not shown here) reveal that a slight modulation of $R_2^{rot}(\tau)$ is limited only to small values of τ, and the deviation of the average relaxation rate from the fast-motional prediction is within 10%. For $D_\perp = 10^4$ s^{-1}, a strong modulation of $R_2^{rot}(\tau)$ is found in the whole explored range of τ values (the variation is of the order of 30−50% depending on the value of $D_{||}$), and the average value of $R_2^{rot}(\tau)$ can differ also by a factor of 2 from that of the fast-motional prediction.

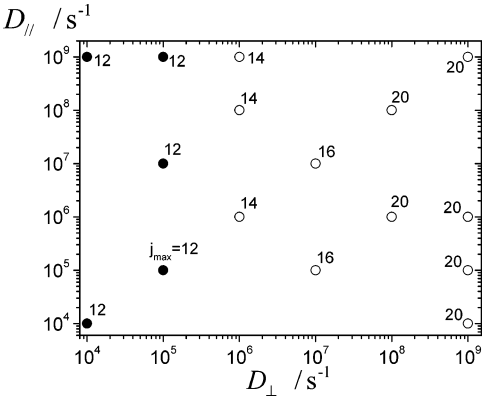

Figure 5. Comparison between full slow-motional and approximated fast-motional approaches to the evaluation of the transverse relaxation rate in QE experiments as due to reorientational dynamics. Calculations are performed for $\epsilon = -6.0$ in the orientational potential, central ring coplanar to the average molecular plane, and for the indicated values of rotational diffusion coefficients. Open circles: situations with negligible deviations from the fast-motional approximation. Full circles: marked deviations from the fast-motional approximation. The maximum rank of basis functions required to achieve numerical convergence with the slow-motional approach, j_{max}, is indicated close to the related circles.

In the specific case, it turns out that the transition between slow-motional and fast-motional regimes is controlled by the rate of molecular reorientations about the transverse axes, while the spinning about the figure axis plays a minor role. Even if the reduction of $D_{||}$ also brings some slow-motional effects, in the specific case only $D_\perp$ determines quantitatively the dynamic regime of the signal relaxation (further calculations with $D_{||}$ down to 10^2 s^{-1} have shown that the partition in Figure 5 is kept). For $D_\perp \geq 10^6$ s^{-1}, we can safely state that the fast-motional approximation holds, while for lower values of $D_\perp$, the full slow-motional treatment has to be employed.

In this regard, we present model calculations of the τ-dependence of $I(2\tau)/I(0)$ and $R_2^{rot}(\tau)$ for $\epsilon = -6.0$ at fixed $D_{||}$ and different values of $D_\perp$. Still we focus on the situation of the C−D bond on the average molecular plane. In Figure 6a, we compare the exact profiles of the echo intensity evaluated in

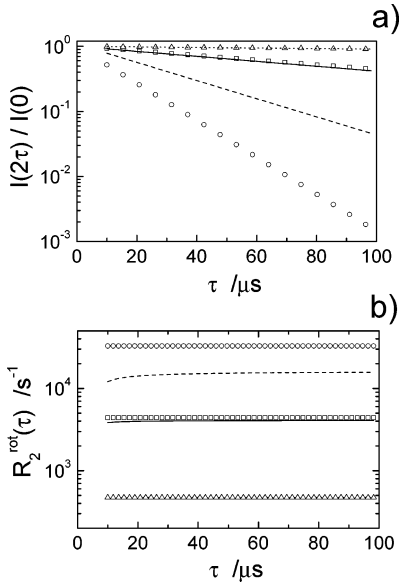

Figure 6. τ-dependence of the (scaled) maximum intensities of the QE (a) and of the transverse relaxation rate (b), as due to reorientational dynamics of the molecule in the nematic phase with director collinear to the magnetic field: comparison between full slow-motional (SM) treatment and fast-motional (FM) limit. Calculations are performed for $\epsilon = -6.0$ in the orientational potential, and for central ring coplanar to the average molecular plane. Other parameters are $D_{||} = 10^5$ s^{-1} (rotational diffusion coefficient about the figure axis), and different values of the rotational diffusion coefficient about transverse axes: $D_\perp = 10^4$ s^{-1} (dashed line for SM, circles for FM), $D_\perp = 10^5$ s^{-1} (solid line for SM, squares for FM) and $D_\perp = 10^6$ s^{-1} (dotted line for SM, triangles for FM).

the slow-motional (SM) context with those from the fast-motional (FM) approximation, for $D_{||} = 10^5$ s^{-1} and for the values $D_\perp = 10^4$ s^{-1} (dashed line for SM, open circles for FM), $D_\perp = 10^5$ s^{-1} (solid line for SM, open squares for FM), $D_\perp = 10^6$ s^{-1} (dotted line for SM, open triangles for FM). In Figure 6b, we show the corresponding profiles of $R_2^{rot}(\tau)$.

Notice that the profiles evaluated in the slow-motional context are sensitive to the regime of rotational motion in terms of magnitude of relaxation rate and features of the profiles. In particular, the profiles in Figure 6b indicate that for fast tumbling (large $D_\perp$) the maximum QE intensity decays monoexponentially with a constant relaxation rate, while in the slow-tumbling regime some deviations from the monoexponential behavior can be found (although little) for small values of τ. In the case of $D_\perp = 10^4$ s^{-1}, the prediction based on the fast-motional approximation completely fails. We remark that even in the slow-motional regime, the (homogeneous) signal relaxation can result apparently monoexponential if monitored on time-scales long enough; in other words, an apparent monoexponential dependence of $I(2\tau)/I(0)$ vs τ can be observed for values of τ long enough (as evident from Figure 6a, b). However, in this case the application of the fast-motional approximation would yield the wrong estimate of the transverse relaxation rate.

As a technical remark, we stress that the rank j_{max} required to reach the convergence in the slow-motional treatment depends strongly on the actual value of $D_\perp$. In Figure 5, these values of j_{max} are indicated close to the related circles; notice the increasing of such a parameter as $D_\perp$ is increased. On the contrary, in the fast-motional approach the required maximum rank of basis functions is entirely controlled by the features of the equilibrium distribution, that is, by the strength-parameter ϵ in the specific case. For $\epsilon = -6.0$, the low rank 12 ensured convergence on the relaxation rate. Thus, because of the easier mathematical handling and the lower dimension of the problem in matrix form, the fast-motional approach is conveniently adopted instead of the full treatment once a partition like that in Figure 5 is established.

Finally, we mention that the analysis illustrated above has been repeated for angular displacements of the C−D bond from the average molecular plane up to 30°. We found no relevant variations about the partition in Figure 5.

Supporting Information Available: Part I contains the estimation of R_2^{DF}, and the demonstration that order director fluctuations can contribute at most for 10% of experimental relaxation rate (see section **2.4**). Part II supplies the derivation of the matrix representation of operator $\tilde{U}$ (see eq 15 of the Appendix) on the basis of rotational Wigner functions. This material is available free of charge via the Internet at http://pubs.acs.org.

References and Notes

(1) Niori, T.; Sekine, F.; Watanabe, J.; Furukawa, T.; Takezoe, H. *J. Mater. Chem.* **1996**, *6*, 1231−1233.

(2) Kentischer, F.; MacDonald, R.; Warnick, P.; Heppke, G. *Liq. Cryst.* **1998**, *25*, 341−347.

(3) Heppke, G.; Moro, D. *Science* **1998**, *279*, 1872−1873.

(4) Prost, J.; Barois, P. *J. Chem. Phys.* **1983**, *80*, 65.

(5) Petschek, R. G.; Wiefling, K. M. *Phys. Rev. Lett.* **1987**, *59*, 343−346.

(6) Tournilhac, F.; Blinov, L. M.; Simon, J.; Yablonski, S. V. *Nature (London)* **1992**, *359*, 621−623.

(7) Domenici, V.; Geppi, M.; Veracini, C. A.; Blinc, R.; Lebar, A.; Zalar, B. *J. Phys. Chem. B* **2005**, *109*, 769−774.

(8) Domenici, V. *Orientational Order and Dynamics of Banana-Shaped and Rod-Like Liquid Crystals by Means of ^{2}H NMR: New Developments*, Ph.D. thesis, University of Pisa, Pisa, Italy, 2005.

(9) Wiant, D.; Gleeson, J. T.; Eber, N.; Fodor-Csorba, K.; Jakli, A.; Toth-Katona, T. *electronic-Liq. Cryst. Communications, Physical Review E* **2005**, *72*, 041712.

(10) Domenici, V.; Fodor-Csorba, K.; Frezzato, D.; Moro, G. J.; Veracini, C. A. *Ferroelectrics*, in press.

(11) Wiant, D.; Stojadinovic, S; Neupane, K.; Sharma, S., Fodor-Csorba, K.; Jakli, A.; Gleeson, J. T.; Sprunt, S. *electronic-Liquid Crystal Communications, Physical Review E*, **2006**, *73*, 030703.

(12) Domenici, V.; Veracini, C. A.; Zalar, B. *Soft Matter* **2005**, *1*, 408.

(13) Luz, Z.; Meiboom, S. *J. Chem. Phys.* **1963**, *39*, 366−372.

(14) Wimperis, S. *J. Magn. Reson.* **1990**, *86*, 46−59.

(15) Veracini, C. A. In *Nuclear Magnetic Resonance of Liquid Crystals*; Emsley, J. W., Ed.; D. Reidel: Dordrecht, The Netherlands, **1985**; Vol. 141.

(16) Redfield, A. G. *Adv. Magn. Reson.* **1965**, *1*, 1.

(17) Polnaszek, C. F.; Bruno, G. V.; Freed, J. H. *J. Chem. Phys.* **1973**, *58*, 3185; Moro, G.; Freed, J. H. *J. Chem. Phys.* **1981**, *74*, 3757.

(18) Domenici, V., Zalar, B., Lebar, A., K. Fodor-Csorba, K., Prampolini, G., Cacelli, I., Veracini, C. A. Unpublished work.

(19) Boden, N.; Kahol, P. K. *Mol. Phys.* **1980**, *40*, 1117.

(20) Heaton, N. J.; Vold, R. R.; Vold, R. L. *J. Chem. Phys.* **1989**, *91*, 56.

(21) Ferrarini, A.; Nordio, P. L.; Moro, G. J. In *The Molecular Dynamics of Liquid Crystals*; Luckhurst, G. R., Veracini, C. A., Eds.; Kluwer Academic: Dordrecht, The Netherlands, 1994; pp 41−69.

(22) Frezzato, D.; Kothe, G.; Moro, G. J. *J. Phys. Chem. B* **2001**, *105*, 1281.

(23) Frezzato, D.; Moro, G. J.; Kothe, G. *J. Chem. Phys.* **2003**, *119*, 6931.

(24) Frezzato, D.; Kothe, G.; Moro, G. J. *J. Chem. Phys.* **2003**, *119*, 6946.

(25) de Gennes, P.-G.; Prost, J. *The Physics of Liquid Crystals*, 2nd ed.; Oxford Universiy Press: New York, 1993.

(26) Frezzato, D.; Moro, G. J.; Tittelbach, M.; Kothe, G. *J. Chem. Phys.* **2003**, *119*, 4060.

(27) Kneppe, H.; Schneider, F.; Sharma, N. K. *J. Chem. Phys.* **1982**, *77*, 3203.

(28) Zientara, G. P.; Freed, J. H. *J. Chem. Phys.* **1983**, *79*, 3077.

(29) Moro, G. *Chem. Phys.* **1987**, *118*, 167; Moro, G. *Chem. Phys.* **1987**, *118*, 181.

(30) Frezzato, D.; Moro, G. J.; Zannoni, C. *J. Chem. Phys.* **2005**, *122*, 164904; Frezzato, D.; Zannoni, C.; Moro, G. J. *J. Chem. Phys.* **2006**, in press.

(31) Domenici, V.; Geppi, M.; Veracini, C. A.; Blinc, R.; Lebar, A.; Zalar, B. *ChemPhysChem.* **2004**, *5*, 91.

(32) Domenici, V.; Czub, J.; Geppi, M.; Gestblom, B.; Urban, S.; Veracini, C. A. *Liq. Cryst.* **2004**, *31*, 91.

(33) Xu, J.; Dong, R. J.; Domenici, V.; Fodor-Csorba, K.; Veracini, C. A. *J. Phys. Chem. B* **2006**, *110*, 9434.

(34) Rose, M. E. *Elementary Theory of Angular Momentum*; Wiley: New York, 1957.

(35) Abragam, A. *Principles of Nuclear Magnetism*; Oxford University Press: New York, 1961.